



## Interfacial parameters in correlation with anti-icing performance

Ba Duc Nguyen, Binh Xuan Cao, Thuy Chi Do, Ha Bich Trinh & Thanh-Binh Nguyen

To cite this article: Ba Duc Nguyen, Binh Xuan Cao, Thuy Chi Do, Ha Bich Trinh & Thanh-Binh Nguyen (2019): Interfacial parameters in correlation with anti-icing performance, The Journal of Adhesion, DOI: [10.1080/00218464.2019.1709172](https://doi.org/10.1080/00218464.2019.1709172)

To link to this article: <https://doi.org/10.1080/00218464.2019.1709172>



Published online: 25 Dec 2019.



Submit your article to this journal [↗](#)



View related articles [↗](#)



View Crossmark data [↗](#)



## Interfacial parameters in correlation with anti-icing performance

Ba Duc Nguyen<sup>a\*</sup>, Binh Xuan Cao<sup>b,c\*</sup>, Thuy Chi Do<sup>d</sup>, Ha Bich Trinh<sup>b</sup>, and Thanh-Binh Nguyen <sup>d</sup>

<sup>a</sup>Tan Trao University, Tuyen Quang, Vietnam; <sup>b</sup>Institute of Research and Development, Duy Tan University, Danang, Vietnam; <sup>c</sup>School of Mechanical Engineering, Hanoi University of Science and Technology, Ha Noi, Vietnam; <sup>d</sup>Thai Nguyen University of Education, Thai Nguyen, Vietnam

### ABSTRACT

In this work, we investigated the correlation between interfacial parameters with anti-icing performance in terms of adhesive strength. Samples with different morphologies and surface energies ranging from superhydrophilic to superhydrophobic were evaluated in relationship with contact angle, contact angle hysteresis, water – glass work of adhesion and ice-glass work of adhesion. Superhydrophobic surfaces with well-textured nanopillars were fabricated via dry etching process following by low-energy chemical compound coating. In addition, flat quartz substrates with low wetting states achieved through UVO expose method were also examined. The results demonstrated the relationship between interfacial parameters and anti-icing performance with important considerations on surface coating material and wetting state. This insight should lead to an understanding of icing phenomena and the design of icephobic surfaces.

### ARTICLE HISTORY

Received 31 October 2019  
Accepted 22 December 2019

### KEYWORDS

Anti-icing; adhesive strength; interfacial parameters; work of adhesion

## 1. Introduction

Ice accretion on fuselage may lead to disastrous crashes due to the lack of lifting force.<sup>[1,2]</sup> Ice accumulation on transportation vehicles, roads, and offshore platforms might cause massive destruction and serious accidents.<sup>[3–6]</sup> In general, anti-icing can be separated into active and passive methods. While active methods involve the removal of ice by using external energy<sup>[7–12]</sup>, passive methods aim to delay the ice formation and remove formed ice without external energy.<sup>[13–15]</sup> The passive methods are usually conducted using the physico-chemical approach based on texturing structure incorporates with low-surface-energy materials coating.

Superhydrophobic surfaces (SHs) have been deeply examined for several decades and believed as promising strategies for ice-phobic materials owing

**CONTACT** Thanh-Binh Nguyen  [nguyenthanhbinh@dhsptn.edu.vn](mailto:nguyenthanhbinh@dhsptn.edu.vn)  Thai Nguyen University of Education, Thai Nguyen, Vietnam

\*Authors contributed equally

This article has been republished with minor changes. These changes do not impact the academic content of the article. Color versions of one or more of the figures in the article can be found online at [www.tandfonline.com/gadh](http://www.tandfonline.com/gadh).

© 2019 Taylor & Francis Group, LLC

to their unique properties in water repellency. Many types of research have reported the advantages of passive anti-icing methods based on superhydrophobic surfaces such as reducing adhesion force<sup>[16–24]</sup> or delaying freezing time.<sup>[25–29]</sup> The low adhesion strength is generally explained by low contact area interaction between liquid droplet and substrate. However, recent studies have proposed that superhydrophobic surfaces are not always the solution for anti-icing due to the wetting transition phenomenon.<sup>[30–34]</sup> In order to facilitate the effective functional icephobic surfaces, various factors have been evaluated to determine their relation with adhesive strength, such as contact angle<sup>[16,21]</sup>, contact angle hysteresis<sup>[16,18,21,35]</sup>, and work of adhesion.<sup>[16,21]</sup> However, the obtained results have indicated the inconsistency in the conclusions.<sup>[30,33]</sup>

Herein, this study investigated the correlation of anti-icing performance in terms of adhesive strength with several interfacial factors such as contact angle, contact angle hysteresis, liquid–solid and solid–solid work of adhesion with some important notes in surface morphology and surface energy. The results were compared with recent related studies and expressed a similar tendency. The originality of this work is the experimental demonstration of the initial interfacial parameters in predicting passive anti-icing properties and proposing the proper factors to determine ice-surface adhesive strength for icephobic surface design.

## 2. Experimental setup

### 2.1. Sample preparation

The experiments were performed on quartz substrates since it is relatively low thermal conductivity and easy to make nanostructures with tailored designs. [Figure 1](#) describes the fabrication process for the nanostructured substrates with different morphologies. First, quartz substrates were cleaned by the ultra-sonication process in Alconox detergent (Sigma-Aldrich Inc., Missouri, United States), followed by cleaning with de-ionized water and drying with nitrogen gas. Clean substrates were then coated with a monolayer of polystyrene (PS) beads (Polysciences Inc., Philadelphia, United States) with 200nm in diameter via the spinning method.<sup>[36]</sup> The size reduction step was controlled by manipulating the concentration of Oxygen plasma and reaction time. The etching process was then conducted by using a gas mixture of  $\text{CF}_4$ :  $\text{H}_2$ :  $\text{O}_2$  bombarding on substrates with an appropriate flow rate. By manipulating the size reduction and etching process, nanostructure was generated directly on the quartz substrate and resulted in a uniform truncated cone shape with a fixed pillar height of 300nm and the top diameter ranging from 30 to 145 nm ([Figure 5](#)). The etched samples were then coated with FOTS (Fluorooctatrchlorosilane, Sigma-Aldrich Inc., Missouri, United States) via vapor phase coating for

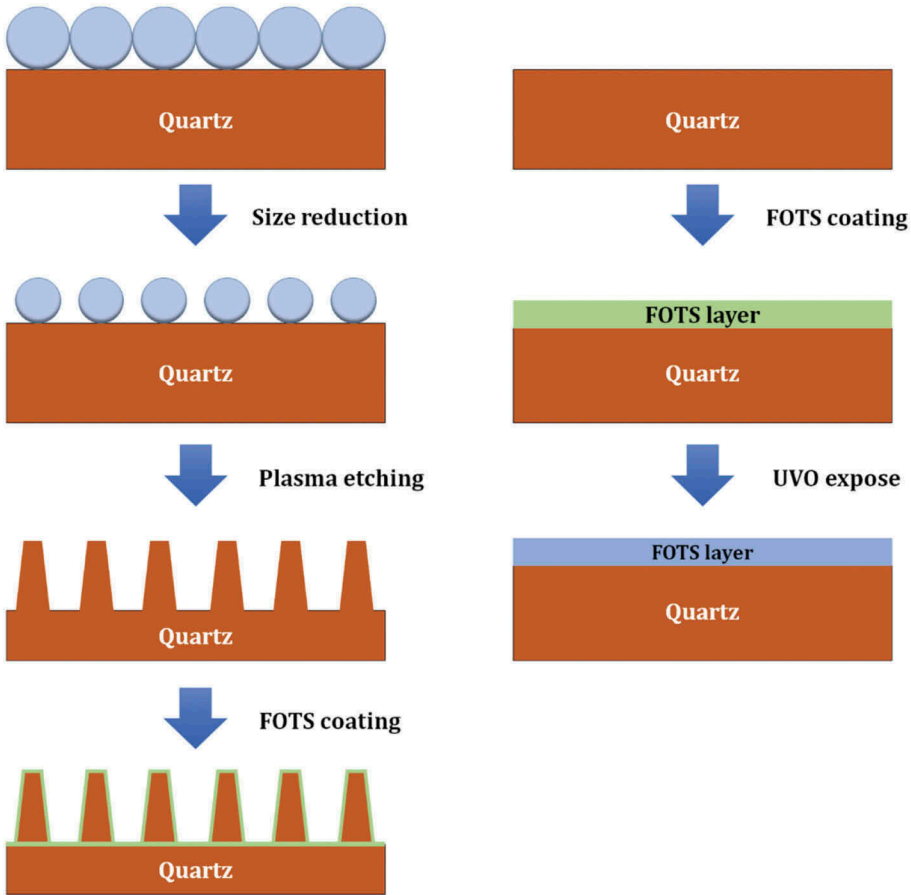


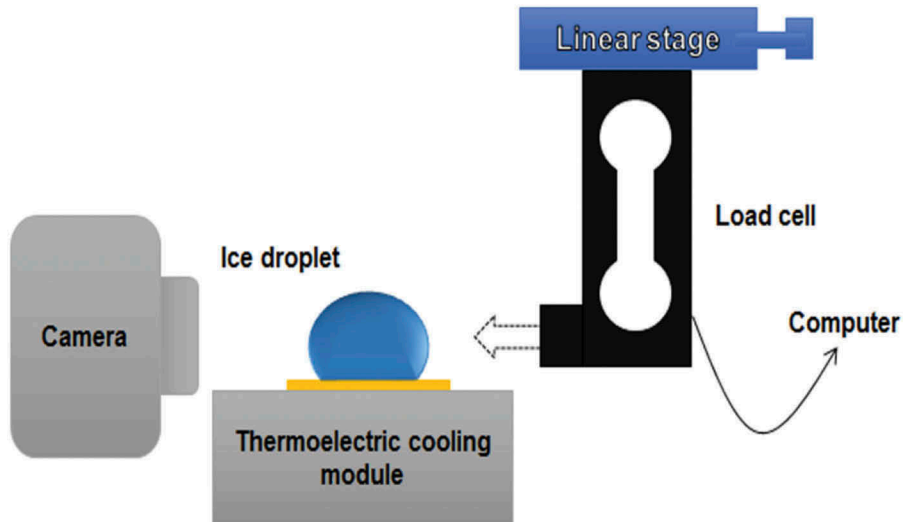
**Figure 1.** The fabrication process of functional surfaces.

1 h, followed by heating at 100°C for another 1 h. After coating, samples had sufficient hydrophobicity, with the contact angle ranging from 132° to 166°. In addition, flat quartz substrates with different surface energies were also fabricated by the UVO treatment process. After coating with FOTS, hydrophobic surfaces were then exposed to UVO flow in appropriate time to generate desired wettability (10° to 90°).

The wettability of samples was measured using a contact angle measurement apparatus (Model DM-50, Kyowa Interface Science Co. Ltd., Saitama, Japan) with 5 $\mu$ L deionized water droplets. Contact angle (CA) and contact angle hysteresis (CAH) were averaged statistically, with ten measurements in independent positions on each sample. [Table 1](#) describes the fabrication details and structural information of all specimens.

**Table 1.** Sample fabrication detail and structural information of specimens.

CA (degree)	CAH (degree)	Fabrication condition	Height (nm)	Top diameter (nm)	Adhesive strength (kPa)	Note
11	24	FOTS – UVO 45 min	-	-	1617	Flat surface
28	19	FOTS – UVO 37 min	-	-	1487	
53	16	FOTS – UVO 30 min	-	-	1372	
72	13	FOTS – UVO 10 min	-	-	1297	
91	11	FOTS – UVO 6 min	-	-	1202	
117	26	Bare quartz glass	-	-	2026	
132	21	Etching – FOTS	300	140	2200	Nano structure
142	12	Etching – FOTS	300	115	2290	
153	4	Etching – FOTS	300	72	626	
159	3	Etching – FOTS	300	55	613	
166	2	Etching – FOTS	300	35	282	

**Figure 2.** Experimental setup for measuring adhesive strength.

## 2.2. Experimental set-up

Ice formation and measurement of adhesion force were performed using a custom-built apparatus as shown in Figure 2. Examined samples were carefully attached to a thermoelectric cooling module by aluminum tape with high thermal conductivity. Firstly, a 5 $\mu$ L deionized water drop was tenderly dropped onto the sample surface and the cooling process was started. The setting temperature of the cooling module was  $-10^{\circ}\text{C}$ . The evaporation and condensation were disregarded because of the short

duration of the experiment (several minutes). The adhesion force was measured using a load cell that was connected to the motorized linear stage, moving at a speed of 50  $\mu\text{m/s}$  and gently pushed an ice droplet horizontally after it solidified. The force exerted on the load cell was recorded by computer software and reached a maximum value as ice droplet was completely detached from the surface, i.e. the adhesive strength between ice and surface. A high-speed camera (Photron Ltd.) was used to record the icing process and measure accurately the real contact area before and after freezing.

### 3. Results and discussion

Recently, some studies have introduced the contact angle as a predictive parameter for determining anti-icing performance.<sup>[16,21,30]</sup> Figure 3 describes the relationship between adhesive strength and contact angle and demonstrates a linear distribution. Our data (blue square) revealed a good correlation with other recent studies as adhesive strength decreased while increasing the liquid-solid contact angle. The lowest value belonged to the superhydrophobic surface while water droplet maintained the Cassie-Baxter wetting state in the whole process.

It was interesting that hydrophobic nanostructure surfaces ( $132^\circ$ ,  $142^\circ$ ) exhibited the extreme high adhesive strength compared to flat and superhydrophobic samples. This mechanism has been mentioned elsewhere and

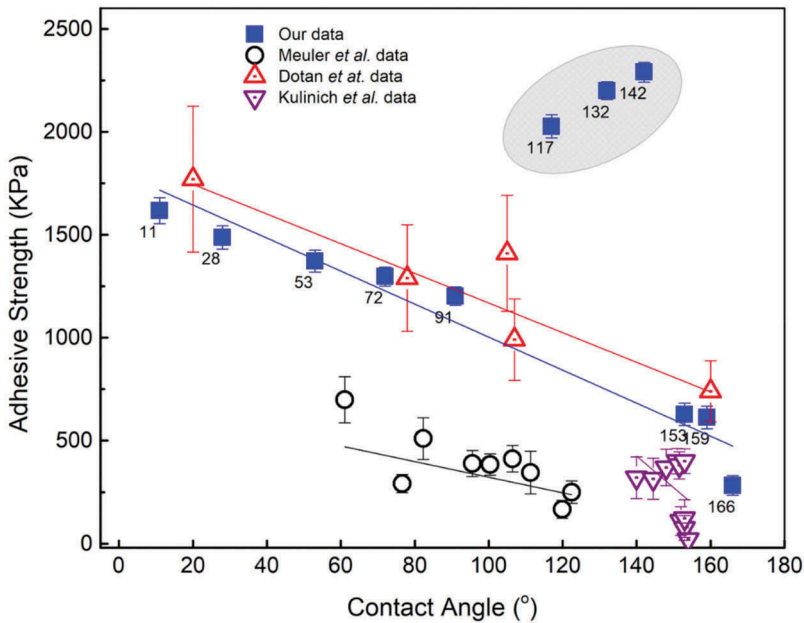


Figure 3. Adhesive strength in correlation with contact angle.

might be explained by the interlocking phenomena while wetting states transformed from Cassie-Baxter to Wenzel state in the cooling process. The transition moment can be observed qualitatively by using the high-speed camera incorporates with a timer. Owing to the low transition energy barrier, water can penetrate deeply into the structure before freezing, facilitating the change of wetting state before solidified. Subsequently, the real ice-solid contact area in these specimens was much larger compared to superhydrophobic specimens and resulted in higher measured adhesive strength.<sup>[30,32,33]</sup> On the opposite side, the linear distribution can be found on flat and superhydrophobic surfaces, illustrating the good correlation between contact area and adhesive strength regardless of smooth or roughness surfaces. The contact angle can be seen as the predictive parameter while we neglect the wetting transition ( $132^\circ$  and  $142^\circ$ ) and divergent surface coating (bare flat surface without FOTS coating).

Figure 4 shows our measurement of contact angle hysteresis plotted against adhesive strength. Currently, several studies have reported that contact angle hysteresis can be seen as the indicated parameter for designing anti-icing surfaces.<sup>[16,18,21,33,35]</sup> Our data were compared with the recent studies and illustrated the relatively same tendency as the adhesive strength increases with the increasing of contact angle hysteresis. The small deviation in linear fitting between studies might be explained by using different materials and surface energies which was governed by chemical compound coating. Same with contact angle, contact angle hysteresis can be also seen as

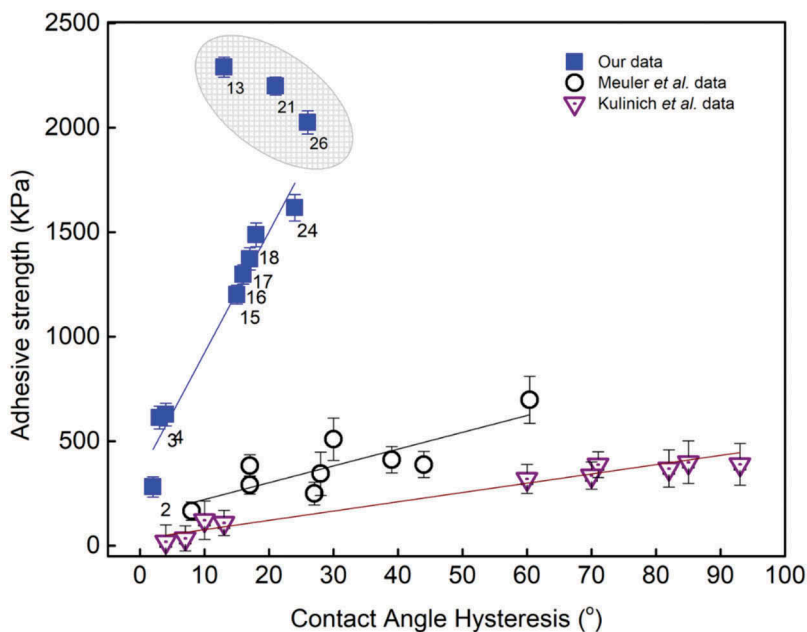
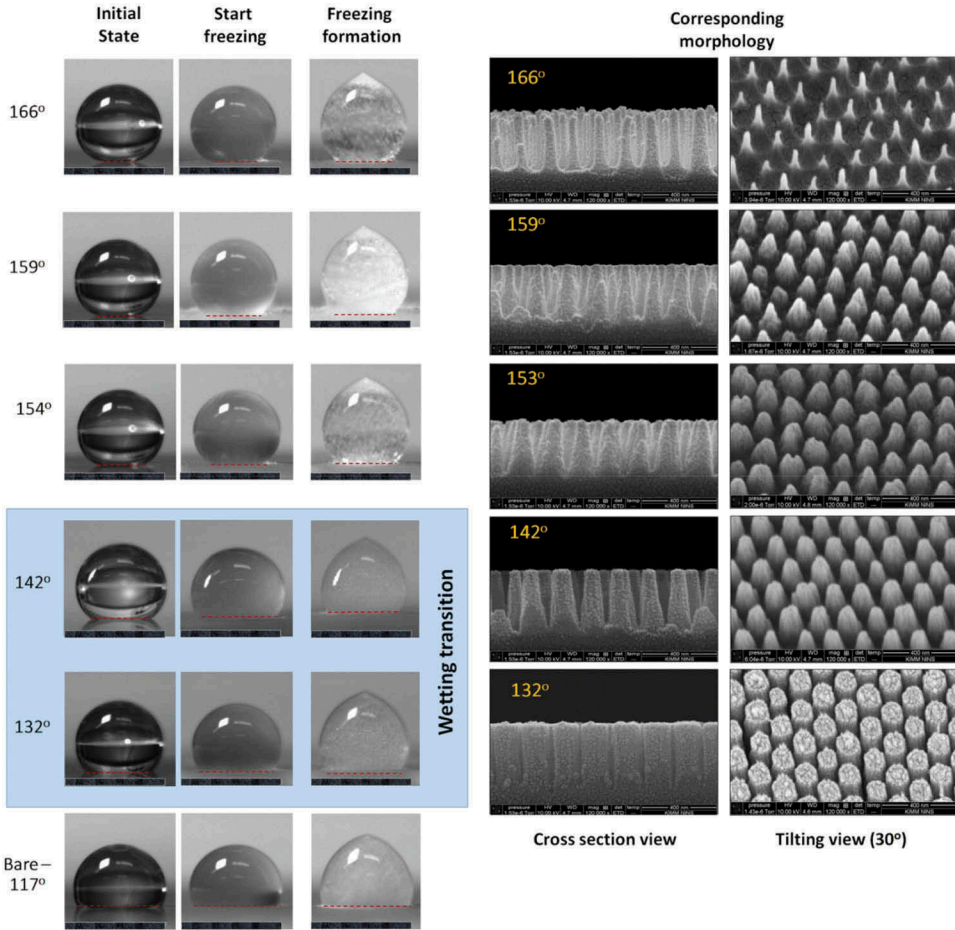


Figure 4. Adhesive strength in correlation with contact angle hysteresis.



**Figure 5.** The icing process and corresponding surface morphology.

the predictive parameter for determining anti-icing performance while neglecting the divergent surface coating and wetting transition effect.

The adhesive strength in correlation with contact angle and contact angle hysteresis revealed the importance of considering wetting transition and surface energy consistency in designing icephobic surfaces. In nanostructure hydrophobic surfaces, water penetrated into space between nano-pillars due to Laplace pressure, incorporated with the sagging effect of the curvature and resulted in the wetting state transformation. In addition, tiny water droplets nucleated inside nanostructure by low temperature can be absorbed by the main droplet subsequently promoted the mechanical locking effect and facilitated unpredictable values. On the opposite side, flat and superhydrophobic surfaces can maintain the stable wetting state at the interface before and after freezing, which ensured the consistent correlation and indicated the predictable values (Figure 5).

The contribution of the work of adhesion in determining anti-icing performance has been examined in the same manner in previous studies. In this work, solid–solid and solid-liquid work of adhesion was investigated individually to figure out their contribution to anti-icing performance. As well known, the liquid-solid work of adhesion can be derived through Young’s equation<sup>[37]</sup>:

$$W = \gamma(1 + \cos \alpha) \quad (1)$$

with  $W$ ,  $\alpha$  and  $\gamma$  are the work of adhesion, the equilibrium contact angle, and liquid-air surface tension, respectively.

It is easy to see that liquid-solid work of adhesion is a linear function of  $\cos \alpha$ . The higher the contact angle we can generate, the lower the work of adhesion we can get. The work of adhesion refers to the work needed to detach two adjacent surfaces, therefore indicates its strong relation with adhesive strength.

Figure 6 presents our measurement of liquid-solid work of adhesion plotted against adhesive strength. Our data were compared with studies of Meuler *et al.*, Dotan *et al.*, Kulinich *et al.*, and illustrated the same tendency as the adhesive strength increased with the increase of work of adhesion. As described in the figure, hydrophobic nanostructure and bare flat samples surprisingly exhibited the extreme high adhesive strength even expressed the relatively low work of adhesion, somehow illustrated the clear separation from the rest. On the opposite side, liquid–solid work of adhesion of superhydrophobic and flat samples

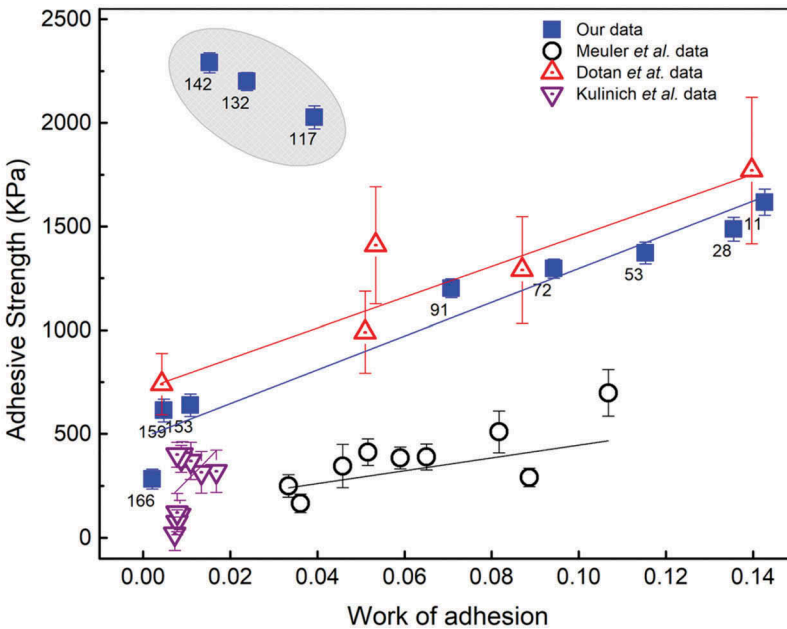


Figure 6. Relationship between adhesive strength and work of adhesion.

presented the linear correlation with adhesive strength, regardless of surface morphology. In the same manner, it was also demonstrated as the predictive parameter for determining anti-icing performance if we dismiss the divergent surface coating and wetting transition effect.

For further discussion, we proposed the new parameter: solid–solid work of adhesion which is governed by inter-molecules interaction at the ice-glass interface. The solid-solid work of adhesion was defined as<sup>[38]</sup>:

$$W = \frac{F^3}{6\pi Ka^3} \quad (2)$$

with  $W$ ,  $F$ ,  $a$ , and  $K$  are the solid-solid work of adhesion, the measured adhesive force, the radius of contact and the elastic constant, respectively. The elastic constant  $K$  is defined in terms of Young's modulus  $E$  and the Poisson' ratio  $\nu$  of two adjacent materials:

$$\frac{1}{K} = \frac{3}{4} \left( \frac{1 - \nu_1^2}{E_1} + \frac{1 - \nu_2^2}{E_2} \right) \quad (3)$$

Young's modulus  $E$  is one of the characteristic properties of solid material and defined as the ratio of stress and strain. The Young's modulus values of ice and quartz glass are 9 and 68 GPa, respectively. The Poisson' ratio  $\nu$  is the negative ratio of transversal and axial strain and very important in determining the mechanical property of each solid material. The Poisson's ratio of ice and quartz glass are 0.33 and 0.334, respectively. The radius  $a$  was measured by using a speed camera equipped with a ruler. We can determine the ice-glass work of adhesion by substituting the elastic modulus value in equation (3) and measuring adhesive force into equation (2). It should be noted here that the solid-liquid work of adhesion can be expressed through Young's equation while solid-solid work of adhesion was derived by a mechanical approach.

Figure 7 illustrates the linear fitting of work of adhesion plotted against adhesive strength in separated meanings: solid-solid (glass-ice) and solid-liquid (glass-water). It was interesting that the experiment results clearly indicated the good agreement between adhesive strength and ice-glass work of adhesion regardless of the surface morphology (flat or roughness) or surface coating (FOTS coating or bare surface). The lowest solid–solid work of adhesion belonged to the 166° sample but the highest value surprisingly corresponded to the 142° sample as the ice-interlocking effect occurred. In the non-structure samples, the highest value belonged to the 11° sample and expectantly decreased by increasing contact angle i.e. decreasing the contact area. This can be seen through the stable wetting formation in the whole cooling process. On the other hand, water droplets on superhydrophobic surfaces maintained the Cassie-Baxter state in the whole process owing to adequate upward pressure, ensured the low ice-solid contact and consequently exhibited low adhesive strength. On the opposite side, the high adhesive strength in hydrophobic nanostructure

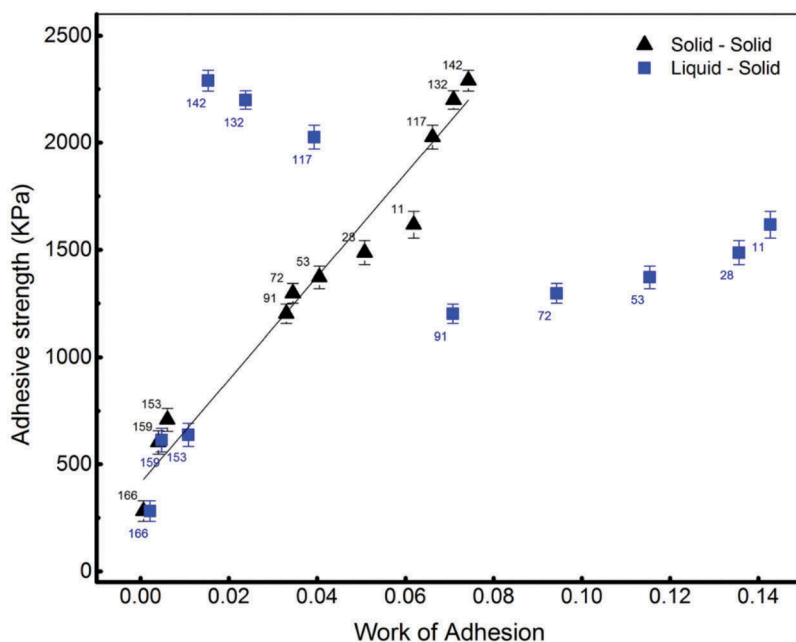


**Figure 7.** Solid-solid and liquid-solid work of adhesion plotted against adhesive strength.

samples was explained by the mechanical locking, resulted in the even higher adhesive strength than smooth surfaces. The pressure difference caused by curvature between neighbor nano-pillars cannot sustain the wetting transition effect and lead to the filling of water inside nanostructure before solidified. From that manner, solid-solid work of adhesion strength, therefore, can be considered as an indicator of adhesive strength.

#### 4. Conclusion

In this work, several liquid-solid interfacial parameters were evaluated in correlation with adhesive strength. The liquid – solid contact angle, contact angle hysteresis, work of adhesion were plotted against the measured adhesive strength and partly illustrated the consistent correlation on superhydrophobic and flat samples with the same chemical compound coating. On the other hand, hydrophobic surfaces exhibited quite high adhesive strength owing to the wetting transition. These experimental results emphasized the need for further consideration in surface energy and wetting transition effect on functional surfaces. Additionally, we proposed a general factor to indicate adhesive strength: solid-solid work of adhesion, which solely depended on solid–solid contact area regardless of surface morphology and surface energy. The lower the work of adhesion we generated, the smaller the adhesive strength we can get. Our study aims to reinforce the understanding of the icing phenomenon and design of icephobic surfaces.

## Acknowledgements

We would like to thank the Department of Nature-inspired Nano Convergence Systems – Nano-Convergence Mechanical Systems Research Division – Korea Institute of Machinery and Materials – South Korea for experimental equipment and valuable supports.

## ORCID

Thanh-Binh Nguyen  <http://orcid.org/0000-0002-5166-7919>

## References

- [1] Laforte, J. L.; Allaire, M. A.; Laflamme, J. State-of-the-Art on Power Line de-Icing. *Atmos. Res.* 1998, 46(1), 143–158. DOI: 10.1016/S0169-8095(97)00057-4.
- [2] Marwitz, J.; Politovich, M.; Bernstein, B.; Ralph, F.; Neiman, P.; Ashenden, R.; Bresch, J. Meteorological Conditions Associated with the ATR72 Aircraft Accident near Roselawn, Indiana, on 31 October 1994. *Bull. Am. Meteorol. Soc.* 1997, 78(1), 41–52. DOI: 10.1175/1520-0477(1997)078<0041:MCAWTA>2.0.CO;2.
- [3] Farzaneh, M.; Ice Accretions on High-Voltage Conductors and Insulators and Related Phenomena. *Philos. Trans. Math. Phys. Eng. Sci.* 2000, 358(1776), 2971–3005. DOI: 10.1098/rsta.2000.0692.
- [4] LANDY, M.; FREIBERGER, A. An Approach to the Shipboard Icing Problem. *Nav. Eng. J.* 1968, 80(1), 63–72. DOI: 10.1111/j.1559-3584.1968.tb05430.x.
- [5] Ryerson, C. C.; Ice Protection of Offshore Platforms. *Cold. Reg. Sci. Technol.* 2011, 65(1), 97–110. DOI: 10.1016/j.coldregions.2010.02.006.
- [6] Tran, P.; Brahimi, M. T.; Paraschivoiu, I.; Pueyo, A.; Tezok, F. Ice Accretion on Aircraft Wings with Thermodynamic Effects. *J. Aircr.* 1995, 32(2), 444–446. DOI: 10.2514/3.46737.
- [7] Boreyko, J. B.; Srijanto, B. R.; Nguyen, T. D.; Vega, C.; Fuentes-Cabrera, M.; Collier, C. P. Dynamic Defrosting on Nanostructured Superhydrophobic Surfaces. *Langmuir.* 2013, 29(30), 9516–9524. DOI: 10.1021/la401282c.
- [8] Cho, H.; Lee, J.; Lee, S.; Hwang, W. Durable Superhydrophilic/Phobic Surfaces Based on Green Patina with Corrosion Resistance. *Phys. Chem. Chem. Phys.* 2015, 17(10), 6786–6793. DOI: 10.1039/C4CP05590J.
- [9] Nguyen, T.-B.; Park, S.; Lim, H. Effects of Morphology Parameters on Anti-Icing Performance in Superhydrophobic Surfaces. *Appl. Surf. Sci.* 2018, 435, 585–591. DOI: 10.1016/j.apsusc.2017.11.137.
- [10] Wang, L.; Teng, C.; Liu, J.; Wang, M.; Liu, G.; Kim, J. Y.; Mei, Q.; Lee, J. K.; Wang, J. Robust Anti-Icing Performance of Silicon Wafer with Hollow Micro-/Nano-Structured ZnO. *J. Ind. Eng. Chem.* 2018, 62, 46–51. DOI: 10.1016/j.jiec.2018.01.022.
- [11] Wang, M.; Yu, W.; Zhang, Y.; Woo, J.-Y.; Chen, Y.; Wang, B.; Yun, Y.; Liu, G.; Lee, J. K.; Wang, L. A Novel Flexible Micro-Ratchet/ZnO Nano-Rods Surface with Rapid Recovery Icephobic Performance. *J. Ind. Eng. Chem.* 2018, 62, 52–57. DOI: 10.1016/j.jiec.2018.01.024.
- [12] Zhang, G.; Hu, J.; Tu, Y.; He, G.; Li, F.; Zou, H.; Lin, S.; Yang, G. Preparation of Superhydrophobic Films Based on the Diblock Copolymer P(TFEMA-r-Sty)-b-PCEMA. *Phys. Chem. Chem. Phys.* 2015, 17(29), 19457–19464. DOI: 10.1039/C5CP02751A.

- [13] Makkonen, L.; Laakso, T.; Marjaniemi, M.; Finstad, K. J. Modelling and Prevention of Ice Accretion on Wind Turbines. *Wind Eng.* **2001**, *25*(1), 3–21. DOI: [10.1260/0309524011495791](https://doi.org/10.1260/0309524011495791).
- [14] MARTIN, C. A.; PUTT, J. C. Advanced Pneumatic Impulse Ice Protection System (PIIP) for Aircraft. *J. Aircr.* **1992**, *29*(4), 714–716. DOI: [10.2514/3.46227](https://doi.org/10.2514/3.46227).
- [15] Palacios, J.; Smith, E.; Rose, J.; Royer, R. Ultrasonic De-Icing of Wind-Tunnel Impact Icing. *J. Aircr.* **2011**, *48*(3), 1020–1027. DOI: [10.2514/1.C031201](https://doi.org/10.2514/1.C031201).
- [16] Dotan, A.; Dodiuk, H.; Laforte, C.; Kenig, S. The Relationship between Water Wetting and Ice Adhesion. *J. Adhes. Sci. Technol.* **2009**, *23*(15), 1907–1915. DOI: [10.1163/016942409X12510925843078](https://doi.org/10.1163/016942409X12510925843078).
- [17] Farhadi, S.; Farzaneh, M.; Kulinich, S. A. Anti-Icing Performance of Superhydrophobic Surfaces. *Appl. Surf. Sci.* **2011**, *257*(14), 6264–6269. DOI: [10.1016/j.apsusc.2011.02.057](https://doi.org/10.1016/j.apsusc.2011.02.057).
- [18] Kulinich, S. A.; Farzaneh, M. How Wetting Hysteresis Influences Ice Adhesion Strength on Superhydrophobic Surfaces. *Langmuir.* **2009**, *25*(16), 8854–8856. DOI: [10.1021/la901439c](https://doi.org/10.1021/la901439c).
- [19] Kulinich, S. A.; Farzaneh, M. Ice Adhesion on Super-Hydrophobic Surfaces. *Appl. Surf. Sci.* **2009**, *255*(18), 8153–8157. DOI: [10.1016/j.apsusc.2009.05.033](https://doi.org/10.1016/j.apsusc.2009.05.033).
- [20] Liu, Q.; Yang, Y.; Huang, M.; Zhou, Y.; Liu, Y.; Liang, X. Durability of a Lubricant-Infused Electrospray Silicon Rubber Surface as an Anti-Icing Coating. *Appl. Surf. Sci.* **2015**, *346*, 68–76. DOI: [10.1016/j.apsusc.2015.02.051](https://doi.org/10.1016/j.apsusc.2015.02.051).
- [21] Meuler, A. J.; Smith, J. D.; Varanasi, K. K.; Mabry, J. M.; McKinley, G. H.; Cohen, R. E. Relationships between Water Wettability and Ice Adhesion. *ACS Appl. Mater. Interfaces.* **2010**, *2*(11), 3100–3110. DOI: [10.1021/am1006035](https://doi.org/10.1021/am1006035).
- [22] Nguyen, T.-B.; Park, S.; Jung, Y.; Lim, H. Effects of Hydrophobicity and Lubricant Characteristics on Anti-Icing Performance of Slippery Lubricant-Infused Porous Surfaces. *J. Ind. Eng. Chem.* **2019**, *69*, 99–105. DOI: [10.1016/j.jiec.2018.09.003](https://doi.org/10.1016/j.jiec.2018.09.003).
- [23] Sarkar, D. K.; Farzaneh, M. Superhydrophobic Coatings with Reduced Ice Adhesion. *J. Adhes. Sci. Technol.* **2009**, *23*(9), 1215–1237. DOI: [10.1163/156856109X433964](https://doi.org/10.1163/156856109X433964).
- [24] Zhang, Y.; Yu, X.; Wu, H.; Wu, J. Facile Fabrication of Superhydrophobic Nanostructures on Aluminum Foils with Controlled-Condensation and Delayed-Icing Effects. *Appl. Surf. Sci.* **2012**, *258*(20), 8253–8257. DOI: [10.1016/j.apsusc.2012.05.032](https://doi.org/10.1016/j.apsusc.2012.05.032).
- [25] Cao, L.; Jones, A. K.; Sikka, V. K.; Wu, J.; Gao, D. Anti-Icing Superhydrophobic Coatings. *Langmuir.* **2009**, *25*(21), 12444–12448. DOI: [10.1021/la902882b](https://doi.org/10.1021/la902882b).
- [26] Tourkine, P.; Le Merrer, M.; Quéré, D. Delayed Freezing on Water Repellent Materials. *Langmuir.* **2009**, *25*(13), 7214–7216. DOI: [10.1021/la900929u](https://doi.org/10.1021/la900929u).
- [27] Wang, H.; He, G.; Tian, Q. Effects of Nano-Fluorocarbon Coating on Icing. *Appl. Surf. Sci.* **2012**, *258*(18), 7219–7224. DOI: [10.1016/j.apsusc.2012.04.043](https://doi.org/10.1016/j.apsusc.2012.04.043).
- [28] Yang, J.; Li, W. Preparation of Superhydrophobic Surfaces on Al Substrates and the Anti-Icing Behavior. *J. Alloys Compd.* **2013**, *576*, 215–219. DOI: [10.1016/j.jallcom.2013.04.060](https://doi.org/10.1016/j.jallcom.2013.04.060).
- [29] Zuo, Z.; Liao, R.; Guo, C.; Yuan, Y.; Zhao, X.; Zhuang, A.; Fabrication, Z. Y. Anti-Icing Property of Coral-like Superhydrophobic Aluminum Surface. *Appl. Surf. Sci.* **2015**, *331*, 132–139. DOI: [10.1016/j.apsusc.2015.01.066](https://doi.org/10.1016/j.apsusc.2015.01.066).
- [30] Chen, J.; Liu, J.; He, M.; Li, K.; Cui, D.; Zhang, Q.; Zeng, X.; Zhang, Y.; Wang, J.; Song, Y. Superhydrophobic Surfaces Cannot Reduce Ice Adhesion. *Appl. Phys. Lett.* **2012**, *101*(11), 111603. DOI: [10.1063/1.4752436](https://doi.org/10.1063/1.4752436).
- [31] Jung, S.; Dorrestijn, M.; Raps, D.; Das, A.; Megaridis, C. M.; Poulikakos, D. Are Superhydrophobic Surfaces Best for Icephobicity?. *Langmuir.* **2011**, *27*(6), 3059–3066. DOI: [10.1021/la104762g](https://doi.org/10.1021/la104762g).

- [32] Kulinich, S. A.; Farhadi, S.; Nose, K.; Du, X. W. Superhydrophobic Surfaces: Are They Really Ice-Repellent? *Langmuir*. 2011, 27(1), 25–29. DOI: [10.1021/la104277q](https://doi.org/10.1021/la104277q).
- [33] Momen, G.; Jafari, R.; Farzaneh, M. Ice Repellency Behaviour of Superhydrophobic Surfaces: Effects of Atmospheric Icing Conditions and Surface Roughness. *Appl. Surf. Sci.* 2015, 349, 211–218. DOI: [10.1016/j.apsusc.2015.04.180](https://doi.org/10.1016/j.apsusc.2015.04.180).
- [34] Zou, M.; Beckford, S.; Wei, R.; Ellis, C.; Hatton, G.; Miller, M. A. Effects of Surface Roughness and Energy on Ice Adhesion Strength. *Appl. Surf. Sci.* 2011, 257(8), 3786–3792. DOI: [10.1016/j.apsusc.2010.11.149](https://doi.org/10.1016/j.apsusc.2010.11.149).
- [35] Sarshar, M. A.; Swartz, C.; Hunter, S.; Simpson, J.; Choi, C.-H. Effects of Contact Angle Hysteresis on Ice Adhesion and Growth on Superhydrophobic Surfaces under Dynamic Flow Conditions. *Colloid Polym. Sci.* 2013, 291(2), 427–435. DOI: [10.1007/s00396-012-2753-4](https://doi.org/10.1007/s00396-012-2753-4).
- [36] Ji, S.; Song, K.; Nguyen, T. B.; Kim, N.; Lim, H. Optimal Moth Eye Nanostructure Array on Transparent Glass Towards Broadband Antireflection. *ACS Appl. Mater. Interfaces*. 2013, 5, 21. DOI: [10.1021/am402881x](https://doi.org/10.1021/am402881x).
- [37] Young, T., III. An Essay on the Cohesion of Fluids. *Philos. Trans. R Soc. London*. 1805, 95, 65–87. DOI: [10.1098/rstl.1805.0005](https://doi.org/10.1098/rstl.1805.0005).
- [38] Pollock, H. M.; Maugis, D.; Barquins, M. The Force of Adhesion between Solid Surfaces in Contact. *Appl. Phys. Lett.* 1978, 33(9), 798–799. DOI: [10.1063/1.90551](https://doi.org/10.1063/1.90551).